

# THE OHIO STATE UNIVERSITY

**The report for Ohio State for the period follows:**

## **INTRINSIC FLOW BEHAVIOR IN A SLURRY BUBBLE COLUMN UNDER HIGH PRESSURE AND HIGH TEMPERATURE CONDITIONS**

Quarter Report

**(Reporting Period: January 1 to March 31, 2001)**

### **Highlights**

- The axial dispersion coefficients of the liquid phase were measured by the steady-state thermal dispersion method. It was found that the axial temperature distribution in terms of  $\ln[(T-T_0)/(T_m-T_0)]$  is almost linear at various gas velocities.
- The axial dispersion coefficient increases significantly with increasing gas velocity. The effect of liquid velocity on the axial liquid mixing is small compared to the effect of gas velocity.
- The study of flow fields and Reynolds stresses at high pressures using a two-dimensional laser Doppler velocimetry (LDV) system was initiated. The LDV system was calibrated under ambient conditions.
- The axial liquid velocity profiles at different gas velocities under ambient conditions for the air-water system were measured using the LDV technique. The regime transition was identified based on the liquid velocity measurement, and the transition superficial gas velocity obtained was about 4 - 6 cm/s in the air-water system.

### **Work Conducted**

#### **1. Study of Axial Liquid-Phase Mixing in High-Pressure Bubble Columns**

##### **Experimental Setup**

The experiments were conducted in a high-pressure column that was 5.08 cm I.D. and 1.0 m in height, including plenum, test and disengagement sections. Three pairs of quartz windows installed on the front and rear sides of each column provide direct visualization of flow behavior inside the column. The columns can be operated up to 22 MPa and 250°C. The details of the high-pressure column are given in Luo et al. (1997).

The axial dispersion coefficients of the liquid phase were measured by the steady-state thermal dispersion method, i.e., introducing heat close to the outlet of the liquid phase and measuring the upstream temperature profile in the liquid. A cartridge heater with an outer diameter of 1.27 cm and a length of 5 cm was used as a source of heat. The maximum heating power was about 370W, and the heater was placed in the center of the column near the gas-liquid outlet. The axial temperature profile within the column was measured by copper-constantan thermocouples placed in the column center at different longitudinal positions, after the steady temperature distribution was attained. The inlet temperatures of liquid and gas were kept constant during the measurement. The maximum temperature difference across the column was controlled within several degrees celsius. A differential pressure transducer was installed to measure the overall gas holdup in the column simultaneously with the temperature measurement, which was required for calculating the axial dispersion coefficient. A perforated plate with 37 square pitched holes of 2.4 mm diameter was used as the distributor. The schematic of the experimental setup is shown in Figure 1.

In this study, nitrogen was used as the gas phase, and water and Paratherm NF<sup>®</sup> heat transfer fluid were used as the liquid phase. The physical properties of Paratherm NF<sup>®</sup> heat transfer fluid ( $\mu_l=0.028$  Pa·s,  $\rho_l=870$  kg/m<sup>3</sup>,  $\sigma=0.029$  N/m at 27<sup>0</sup>C and 0.1MPa) vary with pressure and temperature. Its physical properties at different pressures and temperatures are given in Yang et al. (2000). The liquid is in continuous operation and the liquid velocity varies up to 1.0 cm/s. The gas velocity varies up to 20 cm/s, which covers both the homogenous bubbling regime and heterogeneous bubbling regime.

### **Temperature Distribution**

The measured axial temperature profiles in the column for air-water systems under ambient conditions are shown in Figure 2. It can be seen that the relationships between  $\ln[(T-T_0)/(T_m-T_0)]$  and  $z$  are almost linear at various gas velocities, which indicates that the model assumptions are reasonable. As the superficial gas velocity increases, the axial temperature profile becomes flat, which indicates the increased extent of liquid backmixing at higher gas velocities. The axial dispersion coefficient can be calculated based on the slope of temperature distribution curves and the gas holdup.

### **Comparison with Literature Data**

To verify the validity of the measuring technique, the liquid mixing measurement was first conducted in the air-water system under ambient conditions, and the measured axial dispersion coefficients were compared with the literature data. The effects of gas and liquid velocities on the liquid mixing in the air-water system are shown in Figure 3. It was found that the axial dispersion coefficient increased significantly with increasing gas velocity. Generally, the axial liquid mixing in the nearly uniform dispersed bubbling regime was limited, and the axial dispersion coefficient was small. When the gas velocity was increased, the flow was in the coalesced bubbling or slugging regime, and the non-uniform flow behavior created significant axial liquid mixing. It was also found that the effect of liquid velocity on the axial liquid mixing was small compared to the effect of gas velocity. The axial dispersion coefficient in the air-water system slightly increased with an increase in liquid velocity, especially at low gas velocities. The

measured results were also compared to the available literature data obtained by various methods. Since liquid mixing strongly depends on column size, for comparison purposes, the literature data obtained in different column sizes were converted into the column size used in this study (i.e., 5.08 cm) by using the relationship between the axial dispersion coefficient and the column diameter observed in their studies. If such a relationship was not available in some of the literature studies, the effect of diameter was accounted for by using the following relationship:

$$E_l \propto D^{1.4} . \quad (1)$$

Many studies have proven this relationship capable of predicting the effect of scaleup on liquid mixing (Deckwer et al., 1974; Wendt et al., 1984). The comparison shows that the experimental data obtained in this study using the thermal dispersion technique agree well with most literature data, which further verifies the validity of the measuring technique. It was also found that the data converted from large columns (e.g., >10cm) (Deckwer et al., 1974; Wilkinson et al., 1993) are lower than the experimental data obtained in small columns (Kato and Nishiwaki, 1972; Wendt et al., 1984). This is possibly due to the different mixing behavior between small and large columns. The detailed information from various literature studies used in the figure is provided in Table 1.

## 2. Study of Flow Fields and Reynolds Stresses

### LDV System Setup

To measure the velocity profiles of the liquid phase, a two-dimensional laser Doppler velocimetry system in the backscatter mode was used. Figure 4 shows the schematic of the LDV system. The laser Doppler velocimetry system includes a 300-mW, air-cooled, argon-ion laser system and a beam separator. Two pairs of laser beams with the known wavelengths of 514.5 and 480 nm are generated. The light is transmitted through a fiber optic cable and a probe with 25-cm focal-length lens. This configuration yields 48 fringes with fringe spaces of 3.40 and 3.22  $\mu\text{m}$  and measurement volumes of  $0.164 \times 0.164 \times 2.162$  mm and  $0.156 \times 0.156 \times 2.05$  mm for the 514.5- and 480-nm wavelengths, respectively. The scattered light is collected through the same probe (i.e., backscatter mode) and a detector, and processed by a signal processor.

To measure the turbulent velocities of the liquid phase, neutrally buoyant Pliolite particles,  $1.02 \text{ g/cm}^3$  in density with a size range of 20 - 50  $\mu\text{m}$ , are used as the liquid seeding particles because these kinds of particles are able to follow the liquid flow, even in turbulent conditions. The distortion of laser beams is avoided, since the flat quartz windows installed in the high-pressure cylindrical column are used for the penetration of laser beams.

The application of the LDV technique in bubbly flows is not as trivial as in single-phase flows because of the existence of a dispersed phase. One of the most challenging issues regarding the application of the LDV technique in bubbly flows is proper discrimination among different phases. To reduce the effect of bubbles, the LDV system is operated in

the backscatter mode because the signals obtained in the backscatter mode predominantly represent the liquid phase (Mudde et al., 1998).

All measurements in this study were sampled between 600 and 1200 seconds, and under such a sampling time range, the reliability of the measurement was excellent. The data rate ranged from 10 to 100 Hz. The sampling rate was relatively low because of the system limitation, for example, the low power source of the laser system and relative thickness of the quartz windows. The sampling rate strongly depended on the distance between the measurement point and the wall due to the light scattering caused by bubbles. Ohba et al. (1976) showed that the exponential relationship of the intensity of the scattered light,  $I$ , with the penetration depth of the laser beams,  $l$ , and the gas holdup,  $\varepsilon_g$ , is

$$\frac{I}{I_0} = \exp\left(-\frac{3}{2} \frac{l}{d_b} \varepsilon_g\right), \quad (2)$$

where  $I_0$  is the light intensity without bubbles and  $d_b$  is the distance occupied by a bubble in the direction parallel to the laser beam.

By using one pair of laser beams, the complete radial profile of axial liquid velocity can be obtained, which is referred to as the 1D measurement mode in this study. On the other hand, only half profiles of axial and tangential velocities can be measured using two pairs of laser beams (i.e., 2D measurement mode), because the quartz windows used are not wide enough to allow all the laser beams to pass through.

LDV measurements are currently conducted in the 2-inch, high-pressure column and will also be carried out in the 4-inch vessel. Three pairs of flat quartz windows have been installed on the front and rear sides of the column, and each window is 1.27cm in width and 9.3cm in height. Water is currently used as the liquid phase, and the system is operated in the batch mode. Paratherm NF<sup>®</sup> heat transfer fluid will also be used to study the effect of liquid properties. Figure 5 is the schematic diagram of the experimental setup of the LDV system in the high-pressure bubble column. The effects of operating conditions and design variables, such as pressure, temperature, gas velocity, axial position, column dimension, liquid properties, and internals will be investigated systematically.

### **LDV System Calibration and Test**

Figure 6 shows the experimental results of liquid velocities obtained from both the 1D and 2D measurement modes under ambient conditions. It was found that the flow structure in bubble columns is axisymmetric. The repeatability of measurements is also shown in Figure 6, and the results are reproducible.

Figure 7 compares LDV measurements with literature data reported by Chen et al. (1999). It was found that the results from LDV measurements agree well with those obtained using different measurement techniques.

### **Effect of Gas Velocity**

Figure 8 shows liquid axial velocity profiles measured under ambient conditions at different gas velocities. The liquid axial velocity increases with increasing superficial gas velocity in the central region of the bubble column. The velocity profile becomes steeper at higher gas velocities. There is gross liquid circulation in the column, and the reverse of liquid flow occurs at the point where  $r/R = 0.7$ , which matches other literature studies.

### **Transition of Flow Regime**

Figure 9 shows the effect of gas velocity on axial liquid velocity at the column center. The axial liquid velocity at the center point increases with an increase in the superficial gas velocity; however, the increase in rate varies with gas velocity. At low gas velocities, the center liquid velocity increases quickly with increasing gas velocity. When the gas velocity exceeds a certain value (i.e., about 4.8 cm/s in this study), the increase in rate of center liquid velocity with gas velocity becomes smaller. The point that the increase in rate suddenly changes can be defined as the flow regime transition point.

In order to further verify the transition point identified based on the liquid velocity measurement, gas holdup was also measured using a pressure transducer, and the drift-flux method was used to identify the regime transition.

Figure 10 shows the gas holdup data in the 2-inch column under ambient conditions, and Figure 11 shows the relationship between the drift-flux and the gas holdup. The transition velocity obtained based on the drift-flux method is about 5.8 cm/s, as shown in Figure 10, which agrees with the results obtained from our LDV measurements and the findings in most literature studies, in the range of 4.0 to 6.0 cm/s (Yamashita and Inoue, 1975; Drahos et al., 1992; Hyndman and Guy, 1995; Bakshi et al., 1995).

### **Future Work**

Ohio State's future work will involve the measurement of the axial dispersion coefficients of the liquid phase in bubble columns by the steady-state thermal dispersion method. Work will also be done on quantification of the axial liquid velocity profiles and Reynolds normal and shear stresses.

### **Notations**

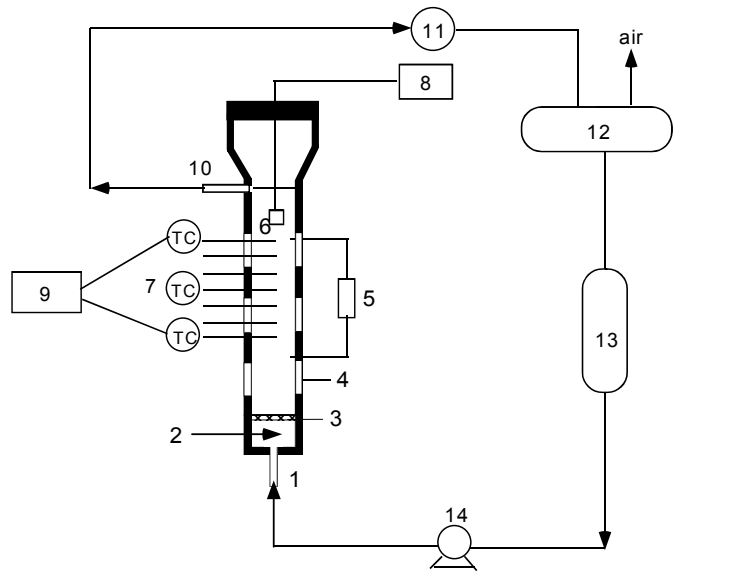
$E_l$	liquid-phase dispersion coefficient, $m^2/s$
$T$	temperature at axial position $z$ , $^{\circ}C$
$T_0$	liquid inlet temperature, $^{\circ}C$
$T_m$	liquid outlet temperature, $^{\circ}C$
$U_l$	superficial liquid velocity, $m/s$
$z$	axial height from the gas-liquid outlet, $m$
$\varepsilon_g$	gas holdup, dimensionless

## References

- Aoyama, Y., K. Ogushi, K. Koide, and H. Kubota, "Liquid mixing in concurrent bubble columns," *J. Chem. Eng. Japan*, **1**, 158 (1968).
- Bakshi, B. R., H. Zhong, P. Jiang, and L.-S. Fan, "Analysis of flow in gas-liquid bubble columns using multi-resolution methods," *Chem. Eng. Res. Des.*, **73**, 608 (1995).
- Chen, J., A. Kemoun, M. H. Al-Dahhan, M. P. Dudukovic, D. J. Lee, and L.S. Fan, "Comparative hydrodynamics study in a bubble column using computer-automated radioactive particle tracking (CARPT)/computed tomography (CT) and particle image velocimetry (PIV)," *Chem. Eng. Sci.*, **54**, 2199 (1999).
- Deckwer, W. D., R. Burckhart, and G. Zoll, "Mixing and mass transfer in tall bubble columns," *Chem. Eng. Sci.*, **29**, 2177 (1974).
- Drahos, J., J. Zahradnik, M. Fialova, and F. Bradka, "Identification and modelling of liquid flow structures in bubble column reactors," *Chem. Eng. Sci.*, **47**, 3313 (1992).
- Holcombe, N. T., D. S. Smith, H. N. Knickle, and W. O'Dowd, "Thermal dispersion and heat transfer in nonisothermal bubble columns," *Chem. Eng. Commun.*, **21**, 135 (1983).
- Hyndman, C. L., and C. Guy, "Gas phase hydrodynamics in bubble columns," *Chem. Eng. Res. Des.*, **73**, 302 (1995).
- Kato, Y. and A. Nishiwaki, "Longitudinal dispersion coefficient of a liquid in a bubble column," *Int. Chem. Eng.*, **12**, 182 (1972).
- Mudde, R. F., J. S. Groen, and H. E. A. Van Den Akker, "Application of LDA to bubbly flows," *Nuclear Engi. And Design*, **184**, 329 (1998).
- Ohba, K., I. Kishimoto, and M. Ogasawara, "Simultaneous measurement of local liquid velocity and void fraction in bubbly flows using a gas laser – Part I: Principle and measuring procedure," *Tech. Rep. Osaka Univ.*, **26**, 547 (1976).
- Wendt, R., A. Steiff, and P. M. Weinspach, "Liquid phase dispersion in bubble columns," *Ger. Chem. Eng.*, **7**, 267 (1984).
- Yamashita, F., and H. Inoue, "Gas hold-up in bubble columns," *J. Chem. Eng. Japan*, **8**, 334 (1975).

**Table 1 Relevant Information from Various References used in Figure 3 regarding Liquid Mixing in an Air-Water System under Ambient Conditions**

Reference	Technique	$U_g$ (cm/s)	$U_l$ (cm/s)	D (cm)	$U_1$ effect	Relation between $E_l$ and $D$
Aoyama et al. (1968)	mass & thermal	0.3~8	0.18~0.62	5.0	No	$D^{1.5}$
Kato & Nishiwaki (1972)	mass	1~25	0.7~1.3	6.6	No	N/A
Deckwer et al. (1974)	mass	1~15	0.71	20	N/A	$D^{1.4}$
Hikita & Kikukawa (1974)	mass	4.3~33.8	0	10	N/A	$D^{1.25}$
Mangartz & Pilhofer (1981)	thermal	0.5~18	0~6	10	No	$D^{1.5}$
Holcombe et al. (1983)	thermal	0~60	0~2	7.8	N/A	$D^{1.33}$
Wendt et al. (1984)	mass & thermal	1.5~30	0.2~4.5	6.3	No	$D^{1.4}$
Wilkinson et al. (1993)	Mass	2~20	0	15.8	N/A	N/A
This work	Thermal	2~20	0.34~1.0	5.08	Small	N/A



- |   |                                |
|---|--------------------------------|
| 1. Liquid inlet                         | 2. Gas inlet                   |
| 3. Perforated plate distributor         | 4. Quartz window               |
| 5. Pressure transducer                  | 6. Heater                      |
| 7. Thermocouples                        | 8. DC power                    |
| 9. Computer and data acquisition system | 10. Gas and liquid outlet      |
| 11. Back pressure regulator             | 12. Gas/liquid separation tank |
| 13. Liquid supply tank                  | 14. Liquid pump                |

**Figure 1 Schematic of Experimental Setup for the Measurement of Liquid-Phase Mixing**



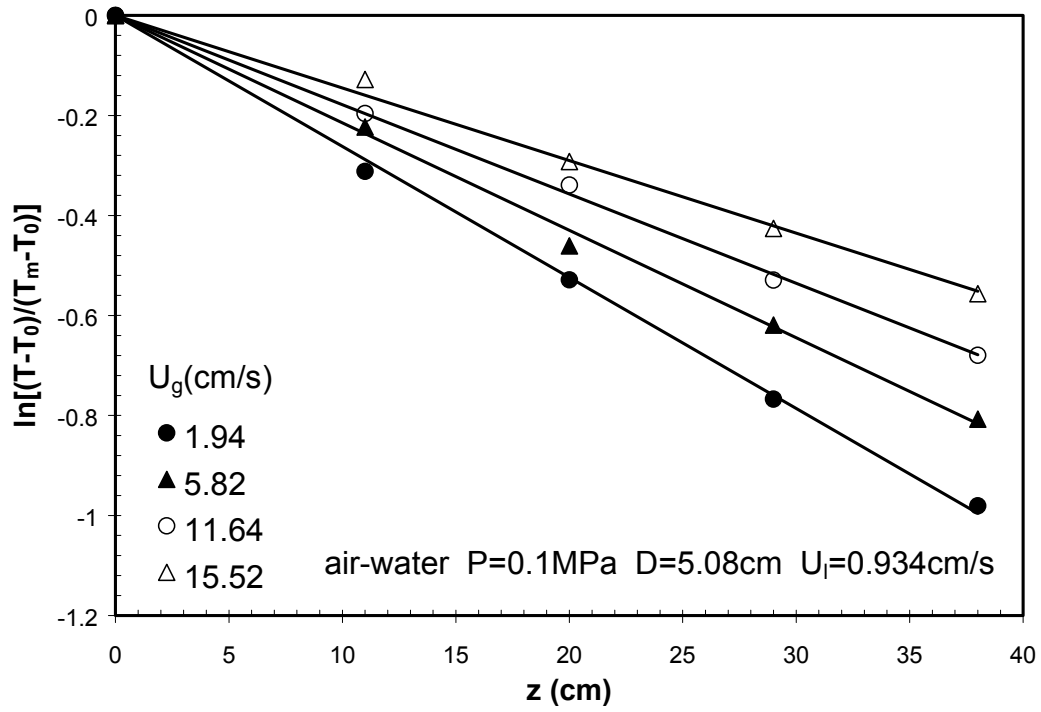


**Figure 2 Typical Temperature Distribution Profiles in the 5.08 cm Column (Air-Water System)**

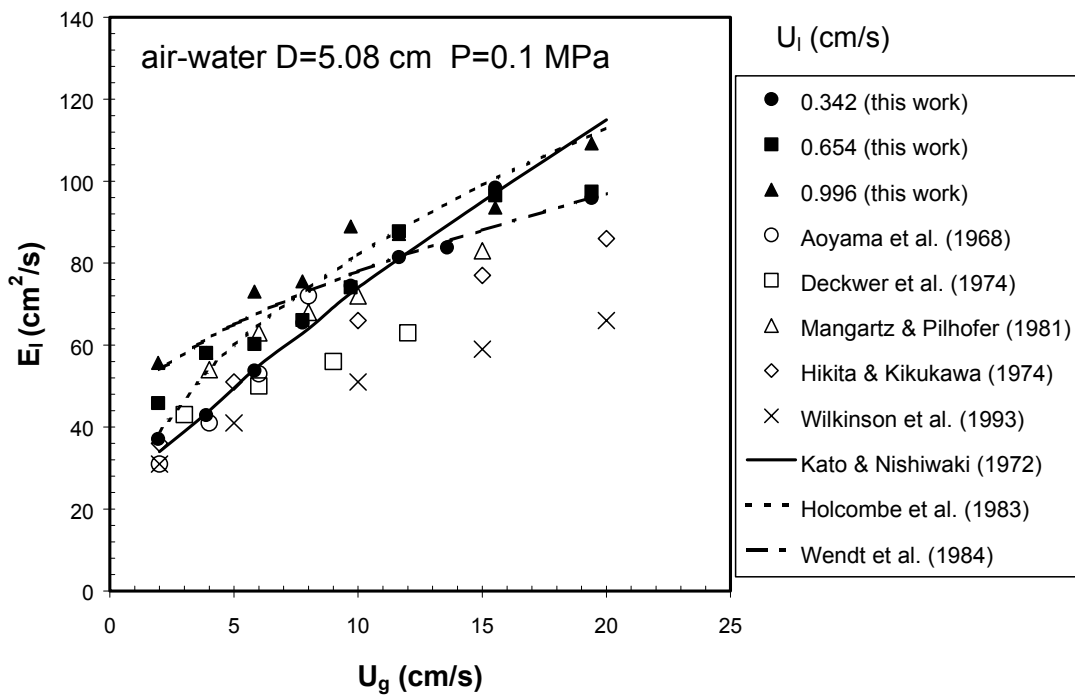
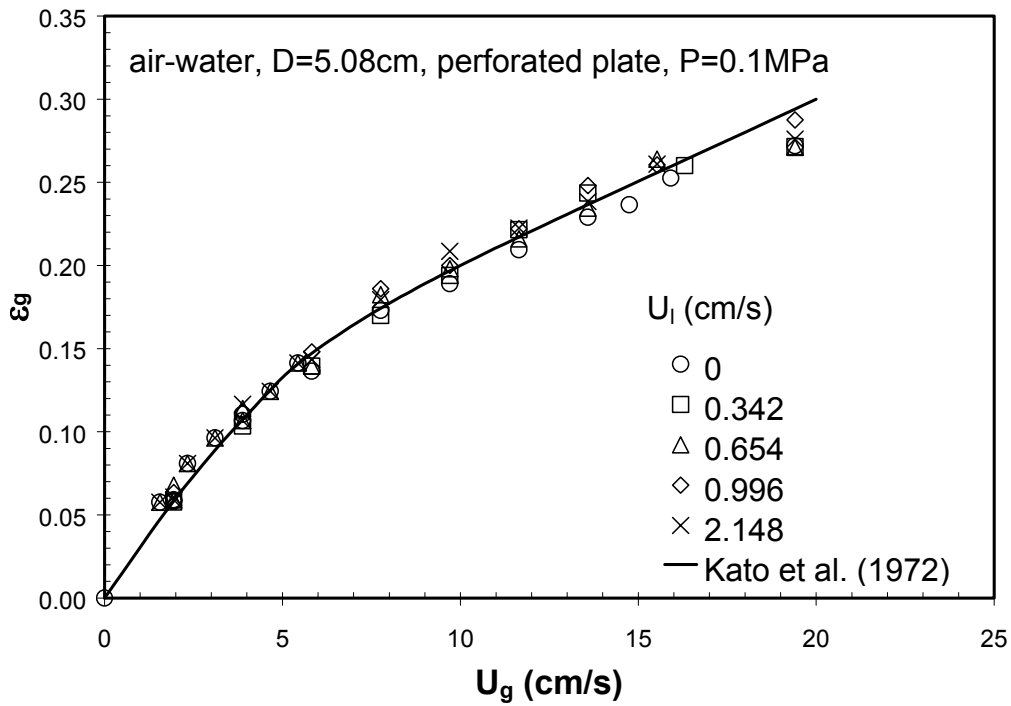
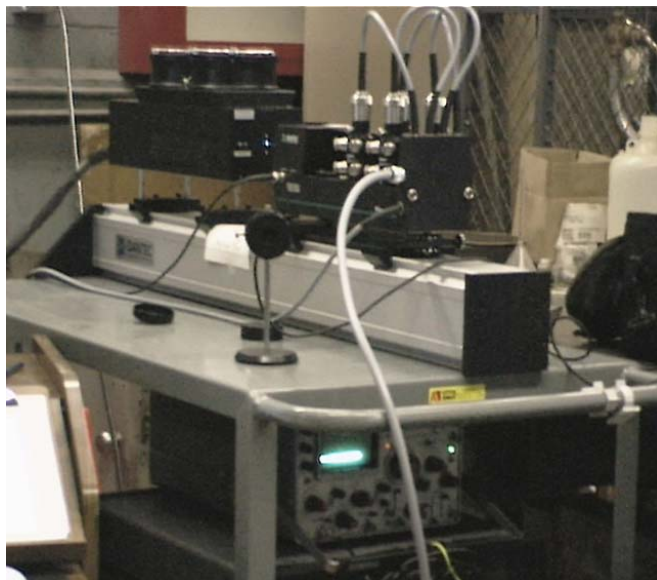
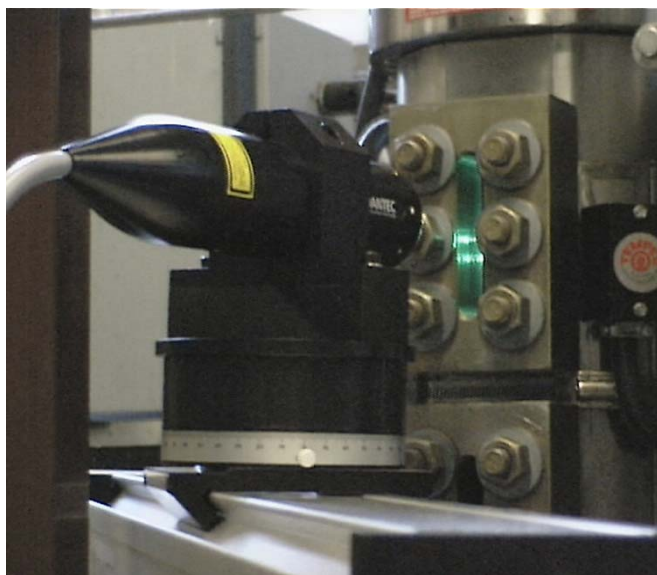


**Figure 3 Comparison of Experimental Data with Available Literature Data for Air-Water Systems under Ambient Conditions**



**(a) LDV system used in this study**



**(b) Laser head and high-pressure bubble column**

**Figure 4 Schematic of LDV Measurement System**

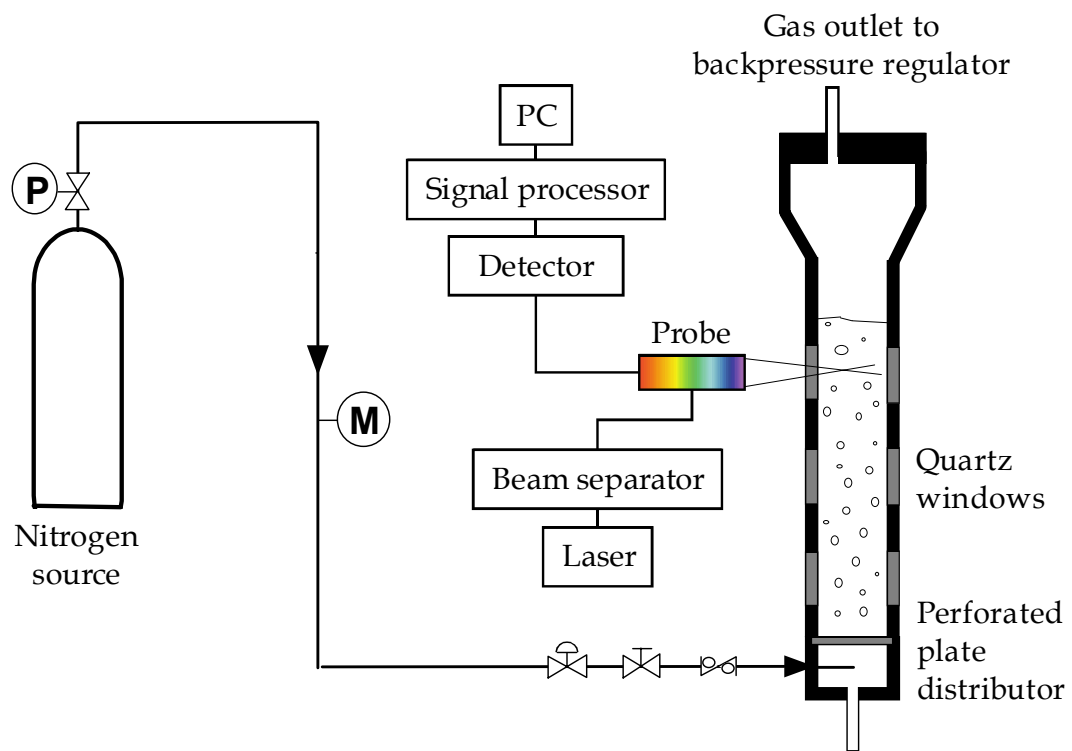


**Figure 5 Schematic Diagram of LDV Measurement in the High-Pressure Vessel**

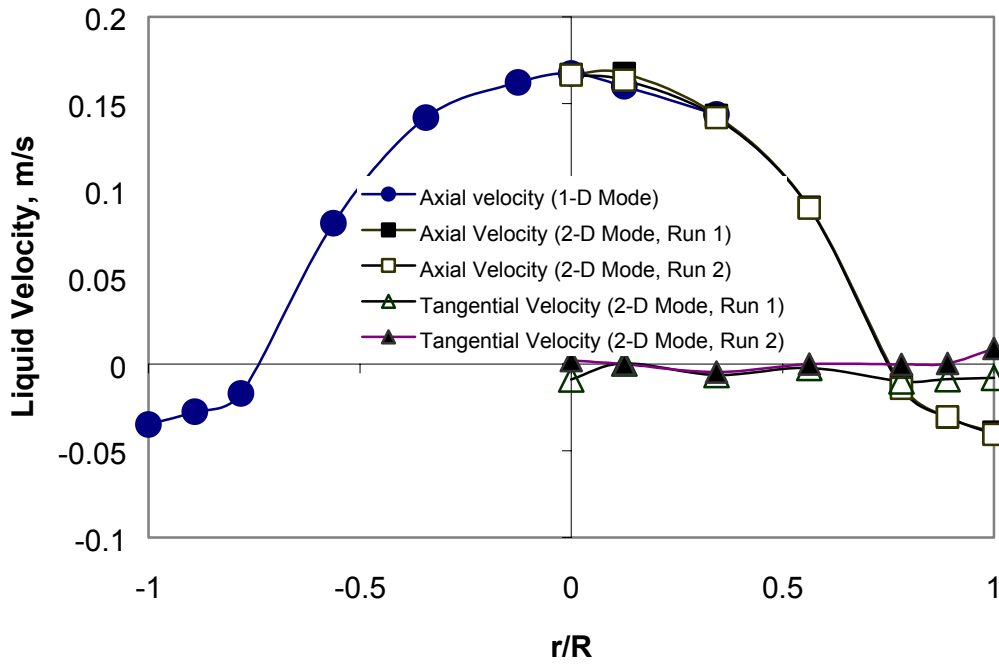


**Figure 6 Comparison of Liquid Velocities measured by 1D and 2D Measurement Modes ( $P=0.1$  MPa,  $D_c=5.1$  cm,  $U_g=2.5$  cm/s)**

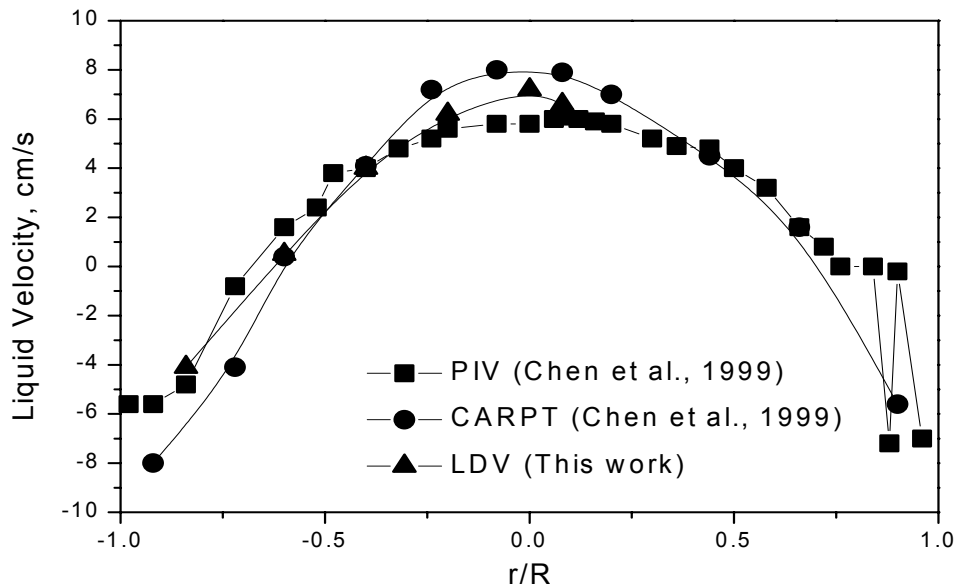


**Figure 7 Comparison of LDV Measurement with Literature Data ( $P=0.1$  MPa,  $U_g=1.9$  cm/s)**

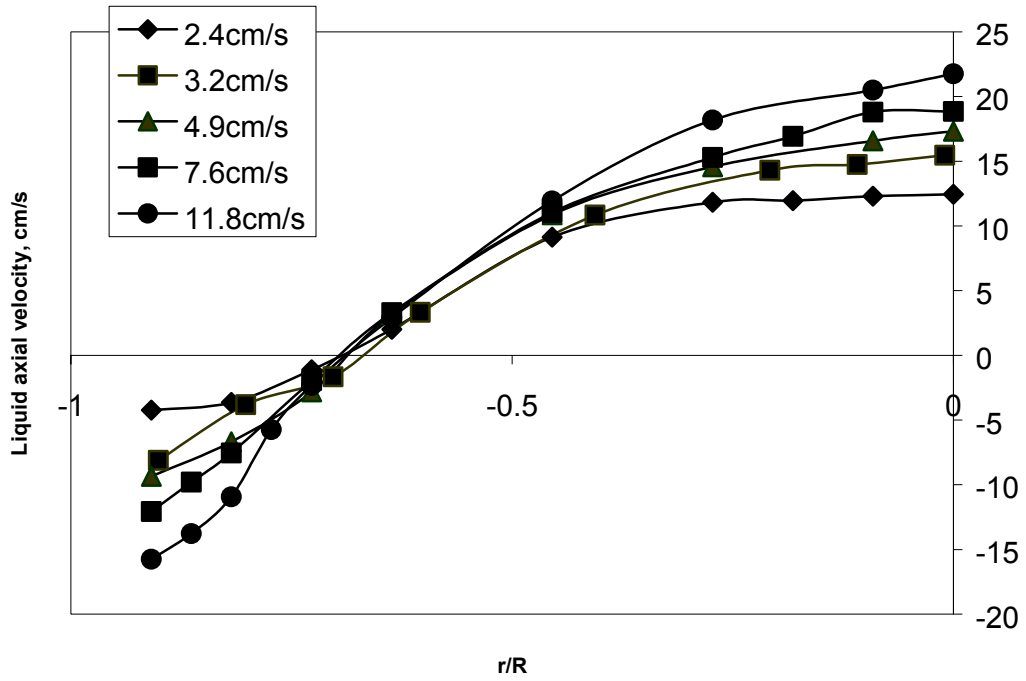


**Figure 8 Axial Liquid Velocity Profiles under Ambient Conditions in the 2-inch Bubble Column**

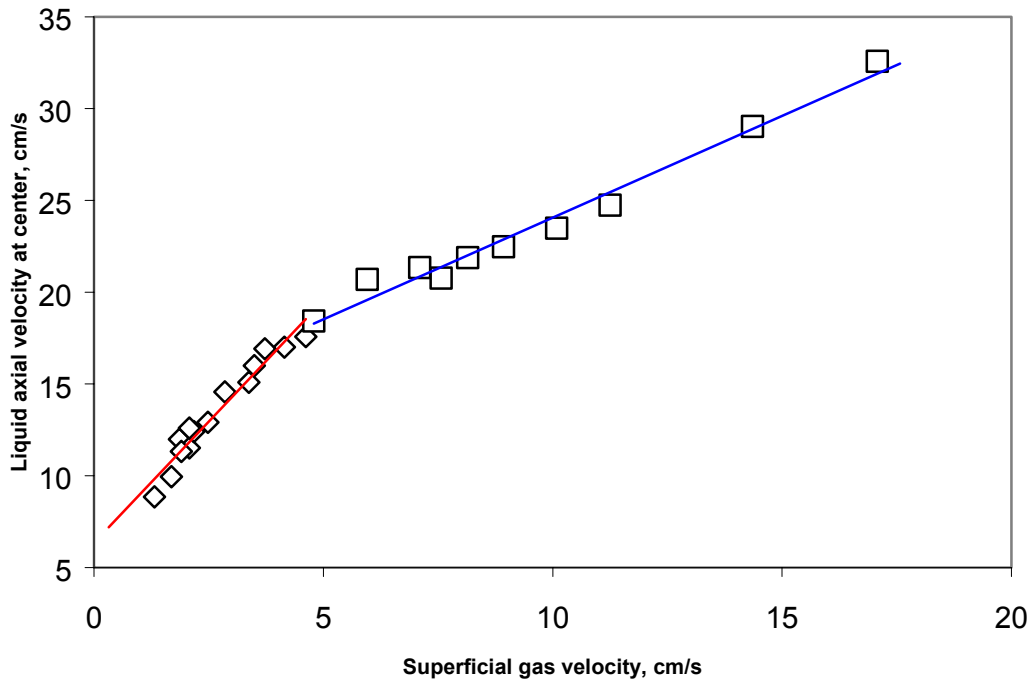


**Figure 9 Effect of Gas Velocity on the Axial Liquid Velocity at Column Center**

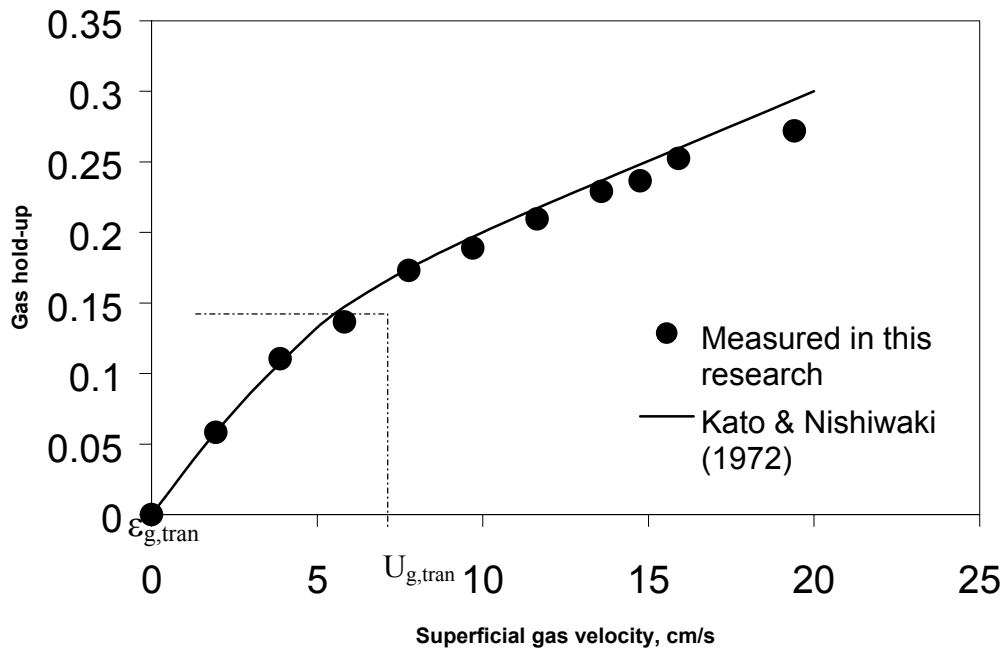


**Figure 10 Effect of Superficial Gas Velocity on Gas Holdup in the 2-inch Bubble Column**  
 ( $U_{g,tran} = 5.8 \text{ cm/s}$ )

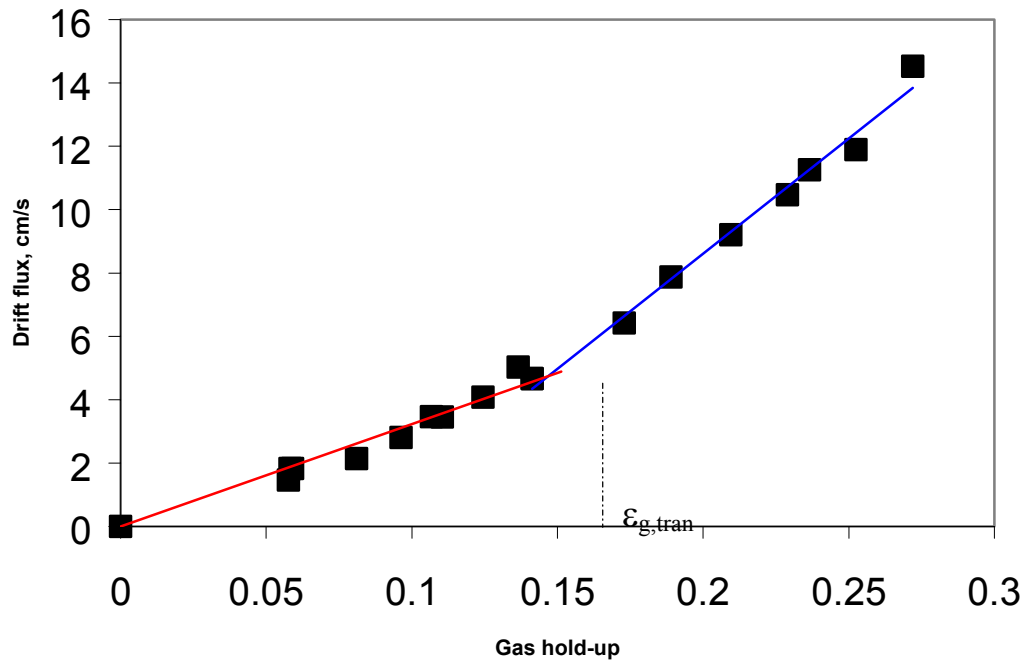


**Figure 11 Identification of Flow Regime Transition based on the Drift-Flux Method**  
 ( $\epsilon_{g,tran} = 0.14$ )